COMMUNICATIONS IN SCIENCE AND TECHNOLOGY
Homepage: cst.kipmi.or.id

Ultrafiltration membranes for dye wastewater treatment: Utilizing cellulose acetate and microcrystalline cellulose fillers from *Ceiba Pentandra*

Romario Abdullah[a], Dinia Astira[a], Utari Zulfiani[a], Alvin Rahmad Widyanto[a,c], Zeni Rahmawati[a], Triyanda Gunawan[a], Yuly Kusumawati[a], Mohd Hafiz Dzarfan Othman[b], Hamzah Fansuri[a,*]

[a]*Department of Chemistry, Institut Teknologi Sepuluh Nopember, Surabaya 60111, Indonesia*
[b]*Advanced Membrane Technology Research Centre (AMTEC), Universiti Teknologi Malaysia, Skudai 81310, Malaysia*
[c]*Department of Applied Chemistry, Shibaura Institute of Technology, Tokyo 135-8548, Japan*

Article History:
Received: 9 December 2023 / Received in revised form: 24 February 2024 / Accepted: 13 May 2024

Abstract

Dye hurts the threat of human health problems and environmental pollution. Microcrystalline cellulose (MCC) based membrane is a good material to be used as an dye separation membrane for having the high hydrophilicity of the membrane. It has been successfully isolated from kapok *(ceiba pentandra)* with characteristic X-ray diffraction patterns and FTIR absorption peaks, which corresponded to the typical peaks of cellulose. The ultrafiltration membrane was made up of a cellulose acetate matrix created using the phase inversion method. Characterization results indicated that the inclusion of MCC derived from kapok led to a reduction in the contact angle from 65 to 52°, and an increase in membrane porosity from 82 to 85%. In the separation of dye, the composite membrane incorporating MCC filler demonstrated superior performance compared to the membrane lacking MCC, manifesting in an elevated water flux from 43 to 84 L/m².h and methylene blue (MB) rejection from 64 to 99%. The use of MCC as a filler in cellulose acetate membranes can enhance the characteristics and performance of the membrane in MB separation.

Keywords: Ultrafiltration membranes; microcrystalline cellulose; kapok; clean water; sanitation

1. Introduction

Kapok (*Ceiba pentandra*) is a significantly abundant biomass in Indonesia, particularly in the tropical regions of Sumatra, Kalimantan, Java, and Sulawesi. This tree thrives in tropical forests, wetlands, and areas with warm climates. In Indonesia, kapok is frequently found in both natural forest areas and plantation forests [1]. Its rapid growth has made it the crucial component of forest ecosystems and is often planted as a shade tree in plantation gardens. Kapok bears various economic and social benefits in Indonesia. Moreover, it holds significant value in scientific development due to its high cellulose content [2-4]. The utilization of kapok as a source of cellulose offers several advantages. Firstly, it grows abundantly in the tropical areas in Indonesia, allowing for local production with a lower environmental impact. Secondly, cellulose fibers from kapok can be applied in various industrial processes, including paper and textile manufacturing, and other products requiring lightweight and water-resistant fiber materials. Sartika et al. [5] reported that kapok is a biomass with a high cellulose content of up to 62.87% and a low lignin content of 4.5%. This characteristic positions kapok as a biomass with great potential for producing cellulose materials.

Cellulose, characterized by a linear structure consisting of D-glucopyranose units linked by (1,4)-glycoside bonds, possesses the molecular formula $(C_6H_{10}O_5)_x$, featuring long, and unbranched chains. Typically white and insoluble in water and certain organic solvents [6], cellulose in nature commonly associates with other polysaccharides such as hemicellulose and lignin, forming the primary components of plant cell walls [7]. With a polymerization degree ranging between 300 and 3000 and a molecular weight spanning 50,000-500,000 g/mol [8], cellulose stands out as the biopolymer with the greatest natural abundance, exhibiting production volumes from 1.0×10^{11} to 1.0×10^{12} tons/year [9,10]. The plentiful presence of cellulose in nature designates it as a renewable material, ensuring a consistent supply of raw materials without any dependencies on fossil resources. Despite its abundance, the utilization of natural cellulose remains relatively limited compared to commercial cellulose [11]. For this reason, there is a need for the advancement of natural cellulose applications to fully harness its potential.

Cellulose has become a very popular material due to its highly porous structure, high specific surface area, large pore

* Corresponding author.
Email: h.fansuri@its.ac.id
https://doi.org/10.21924/cst.9.1.2024.1345

volume [12], non-toxicity, affordability, biodegradability, as well as its high strength, purity, and porosity [13]. Microcrystalline cellulose (MCC) is a type of cellulose with high crystallinity that has experienced high demand as a supporting material for cellulose-based catalysts. When used as a filler in membranes, MCC increases both strength and hydrophilicity, leading to improved membrane performance [14]. Additionally, the incorporation of MCC can reduce the production costs of membranes and contribute to the development of more eco-friendly membranes by using natural fibers or biomass [15]. In the development of membrane technology, various biomasses have been utilized as the sources of microcrystalline cellulose for membrane production, including dong ling cao [16], fruit waste [17], bagasse [18], and empty fruit bunches of oil palm [19]. The high cellulose content and low lignin in kapok make it a biomass with significant potential for microcrystalline cellulose production. The use of MCC as a filler in membranes has been previously reported by Pramono et al. [19] who developed a PVDF/MCC composite membrane using MCC sourced from empty oil palm fruit bunches for separating humic acid. The addition of MCC increased water flux from 16.76 to 27 L/m^2.h and humic acid rejection up to 99%. Additionally, the use of MCC filler-based composite membranes for processing humic acid has been reported by Nazri et al. [14] who added commercial MCC to PES membranes. Experimental results indicated that the addition of MCC could increase water flux up to 115.67 LMH and rejection up to 97.16%. These two reports highlighted MCC as a material with significant potential for use as a filler in membranes. Therefore, this research focuses on producing MCC from kapok and using it as a filler in cellulose acetate membranes for treating dye wastewater, particularly methylene blue. Several parameters studied in this research included the weight percent of MCC in the composite membrane and the test duration for membrane performance in MB separation.

2. Materials and Methods

2.1. Materials

The materials used in this study were kapok (*Ceiba petandra*), Avicel PH 10, ethanol (Smartlab, 96%), toluene (Smartlab, 99%), sodium hydroxide (Merck, 99%), hydrogen peroxide (Merck, 30%), hydrochloric acid (Smartlab, 37%), cellulose acetate (Sigma Aldrich, 99%), dimethylformamide (Merck, 99.5%), and methylene blue (Merck, 99%).

2.2. Isolation of microcrystalline cellulose from kapok

The process of isolating microcrystalline cellulose (MCC) from kapok was carried out using an alkalization method modified from the work of Holilah et al. [20], which is divided into four stages: dewaxing with toluene-ethanol solvent, delignification with 5% NaOH, bleaching with mixture 5% NaOH and 3% H_2O_2, and the last process, hydrolysis with 3.5 N HCl.

2.3. Synthesis of ultrafiltration membrane

The ultrafiltration membrane was made from cellulose acetate polymer with MCC filler from kapok, the manufacturing process of which was modified from the work of Asiri et al. [21]. Membrane manufacture started by dispersing MCC in dimethylformamide solvent using the ultrasonication method for 30 minutes. Then, the cellulose acetate polymer was used with a concentration of 12%. Next, the mixture was stirred for 4 hours at 75ºC and continued for 8 hours at 60ºC. The dope solution formed then removed air bubbles by leaving it for 12 hours. Subsequently, the membrane printing procedure was conducted through the phase inversion method, involving the pouring and casting of the dope solution onto a glass plate, followed by placement in a coagulant bath containing aqua DM. The weight percentage of MCC in membrane fabrication was altered, ranging from 0.5% to 1% and 1.5%.

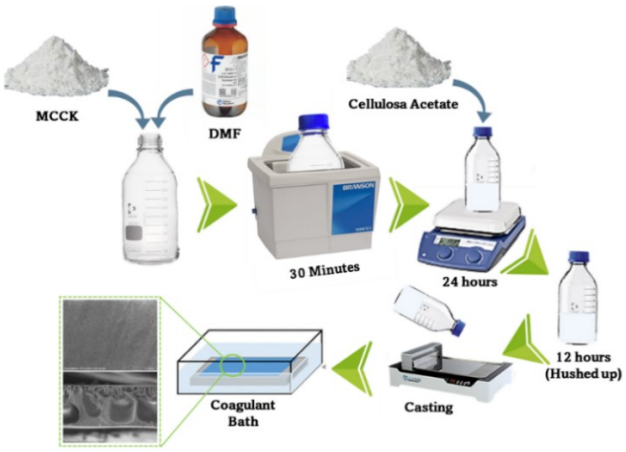

Fig. 1. Process for making cellulose acetate/MCC composite membranes

2.4. Characterizations

The characterization of MCC extracted from kapok involved the utilization of X-ray Diffraction (XRD) to assess the crystal structure's characteristics. The XRD apparatus employed was an X'Pert PANalytical with a Cu Kα source (λ = 1.5406 Å). Measurements were conducted at 2θ angles between 5 and 50 degrees with a step size of 0.01 degrees. To analyze the functional groups within the MCC structure, Fourier Transform Infrared (FTIR) was employed in which its spectra were captured using a Thermo Scientific Nicolet IS10 across wave numbers ranging from 500 to 4000 cm^{-1}. The thermal stability of MCC was examined using the PerkinElmer Pyris 1 TGA Thermogravimetric Analyzer. The morphological analysis of MCC was performed using the Hitachi Flex SEM100.

The characteristics of the composite membrane containing MCC filler from kapok were examined using various instruments. To assess membrane hydrophilicity, contact angle measurements were conducted with a 3D OM vhx-500. The membrane's functional groups were analyzed through FTIR (Thermo Scientific Nicolet IS10) across wave numbers ranging from 500 to 4000 cm^{-1}. Membrane porosity was determined using the gravimetric method. The surface morphology and cross-section of the membrane were scrutinized using the SEM Hitachi Flex SEM100.

2.5. Performance test on dye wastewater treatment

The composite membrane underwent testing to assess its effectiveness in terms of permeability and rejection of methylene blue dye. The ultrafiltration testing procedure was conducted

using a crossflow system at a laboratory scale, employing a peristaltic pump with a water flow rate of 100 ml/minute for 30 minutes. The effectiveness of the composite membrane was assessed by analyzing both water flux and its rejection of MB. The calculation of water flux was determined using Equation 1.

$$J_v = \frac{V}{A\ x\ t} \quad (1)$$

with: J_v = Flux ($L \cdot m^{-2} \cdot h^{-1}$), V = Permeate volume (L), A = Surface area of the membrane (m^2) and t = Time (hours)

The assessment of the membrane's effectiveness in rejecting MB dye involved the use of a 5 $mg \cdot L^{-1}$ concentration of MB solution. The composite membrane, exhibiting superior performance, served as the test medium with variations in MB concentration. The concentration of the resulting permeate was measured using UV-752N Ultraviolet-Visible Spectroscopy (UV-Vis) at a wavelength of 664 nm. The membrane's rejection capacity was determined using Equation 2.

$$R = \frac{(C_f - C_p)}{C_f} x100\% \quad (2)$$

with: R = Rejection percentage (%), C_f = Feed concentration ($mg \cdot L^{-1}$), and C_p = Permeate concentration ($mg \cdot L^{-1}$).

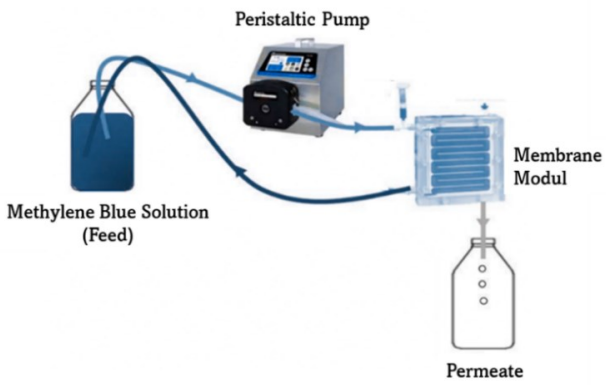

Fig. 2. Membrane performance testing process in the separation of MB

3. Results and Discussion

3.1. Synthesis and characterization of MCC from Kapok

The results of the XRD analysis as shown in Fig. 3(a) showed that the diffractogram of the raw kapok material indicated an intensity peak that was almost similar to the effects of MCC isolation from kapok (MCCK) at 2θ = 15.2 and 22.5°. However, the diffractogram shown still had wide diffraction peaks [22], and there was a peak at 2θ = 43.6°, which was not a cellulose peak. On the other hand, the diffractogram of MCCK showed the typical peaks for cellulose, which was sharper and higher compared to the raw kapok material. The typical cellulose peak in MCCK was 2θ = 15-16, 22.5, and 34.6°. The differences in peak position and intensity prove the removal of lignin and hemicellulose as a characteristic of the amorphous phase after the alkalization process [23,24]. Holilah et al. [20] also reported that the increase in intensity at the peak of 22.6° is the main indicator to confirm the formation of MCC. In addition, the suitability of the MCCK diffractogram with commercial MCC (MCCC) indicates the success of the MCC isolation process from kapok.

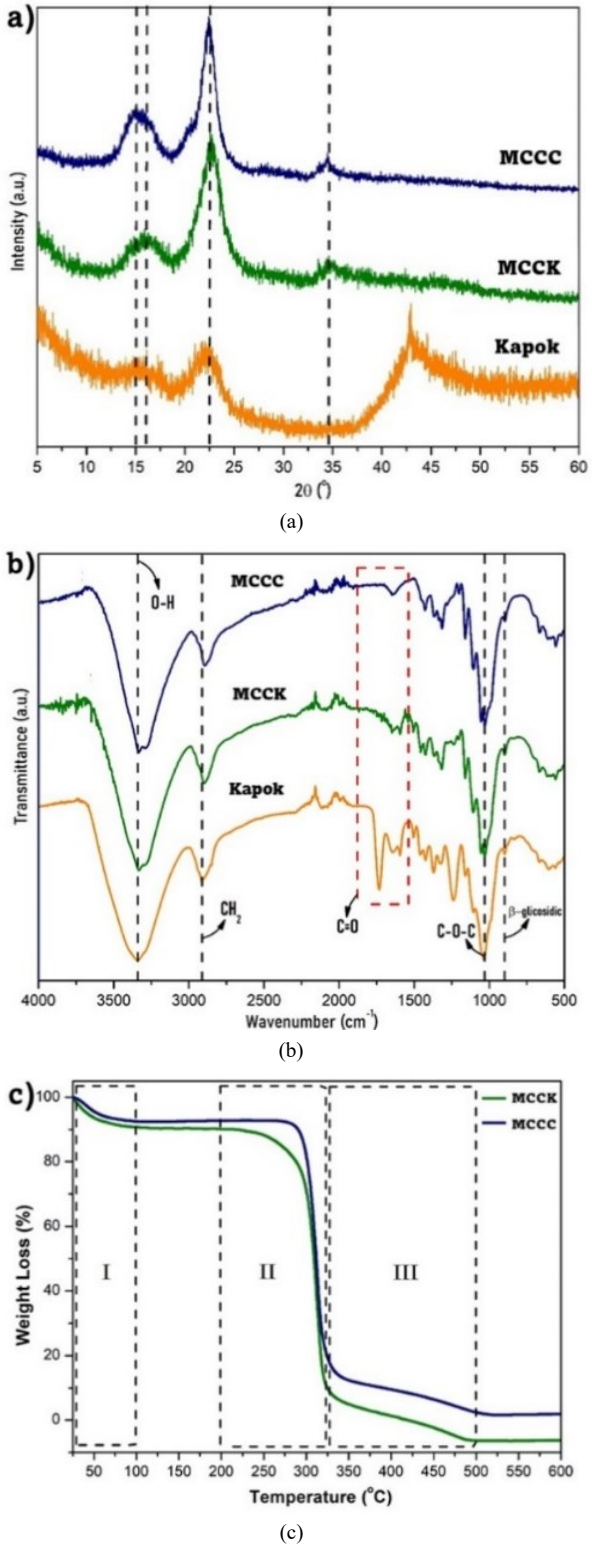

Fig. 3. (a) X-Ray diffractogram, (b) FTIR spectra, and (c) Thermogram of MCCK and MCCC

The FTIR spectrum as depicted in Fig. 3(b) revealed the absorption bands present in the raw material spectra of Kapok and MCCK. Both spectra suggested the existence of cellulose

content, as evidenced by the appearance of an absorption peak at 896 cm^{-1}, indicating the presence of a C-O group in the 1,4-glycoside bond [25,26]. Additionally, the identification of the C-O-C group in the pyranose ring unit was manifested by a peak at 1029 cm^{-1} [27]. The absorption peaks at 2895 and 3332 cm^{-1} further indicated the presence of C-H and O-H groups in the cellulose structure, respectively [28]. Noteworthy differences were observed in the raw kapok material spectra. The appearance of a peak at 1732 cm^{-1} indicated stretching vibrations due to the C=O group, signifying the presence of lignin compounds. The application of alkalization treatment with NaOH resulted in the disappearance of this peak in the MCC spectrum, indicating the successful isolation of MCC from kapok. This was further corroborated by the alignment of absorption peaks between MCCK and MCCC.

The TGA analysis results revealed that the MCCK thermogram exhibited a decomposition pattern consistent with commercial MCC. Both thermograms displayed three stages of decomposition, as depicted in Fig. 3(c). The initial decomposition, occurred at a temperature of 50 - 100°C, was attributed to the physical removal of water adsorbed in the MCC. The second decomposition within the temperature range of 200 – 325°C indicated the ongoing cellulose degradation process. The final decomposition process took place at a temperature of 325 – 500°C, signifying the oxidation process of carbon residues resulting from cellulose degradation [20]. MCCK and MCCC exhibited stability up to 313°C, which aligned with the typical decomposition temperature of cellulose. Carrier et al. [29] stated that cellulose generally undergoes decomposition within the temperature range of 300-350°C.

SEM analysis in Fig. 4 showed some differences in the surface morphology of MCC before and after the alkalization process. The kapok raw material (Fig. 4(a)) offerred long fibers with rough surfaces. Meanwhile, MCC (Fig. 4b-4d) showed a change in fiber length by becoming smaller. The difference in fiber size was caused by the hydrolysis process, which impacted the breaking of the β-1,4-glycosidic bonds connecting the cellulose chains [30,31]. Based on measurement analysis using Image-J software, the MCCK diameter was up to 7.82 µm with an average diameter value of 14,445 µm.

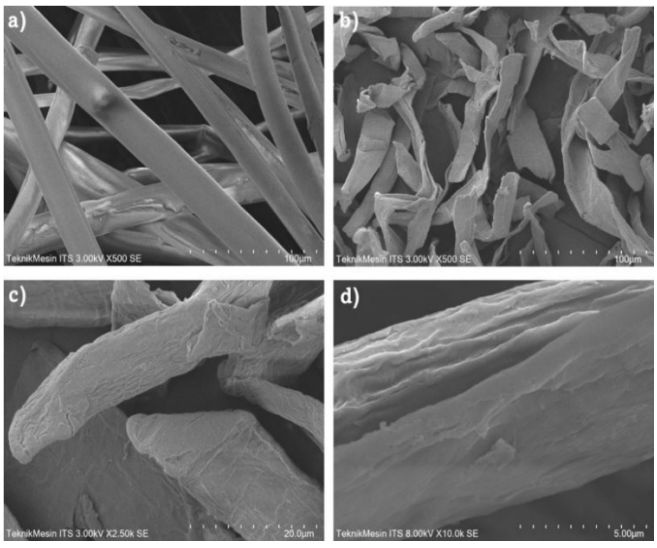

Fig. 4. Morphological analysis (a) kapok raw materials, and (b-d) MCCK

3.2. Fabrication and characterization of membranes

The FTIR analysis of the CA-MCCK membrane displays spectra akin to those of pristine cellulose acetate membranes (Fig. 5). The emergence of an absorption peak at 901 cm^{-1} indicated the presence of C-O vibrations in the 1,4-glycoside bonds connecting cellulose monomer units [32]. Additionally, the appearance of an absorption peak at 1035 cm^{-1} signified the occurrence of asymmetric C-O-C stretching vibrations in the pyranose ring unit, which formed the framework of the cellulose structure [33]. The presence of CH_2 and O-H groups in the membrane was revealed by absorption peaks at 1367 and 3401 cm^{-1}, respectively [32,34]. The acetyl group in the cellulose acetate structure was indicated by an absorption band at 1737 cm^{-1}, denoting the presence of symmetric and asymmetric stretching vibrations of the carbonyl group (C=O) from the ester group [35].

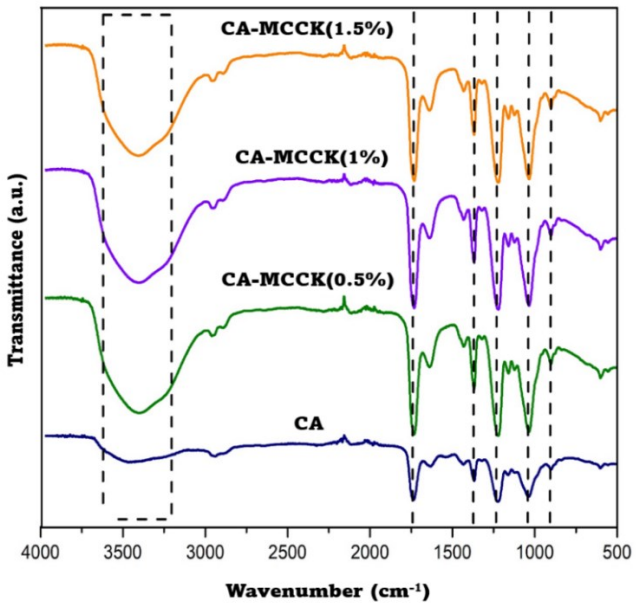

Fig. 5. FTIR spectra of CA-MCCK membrane and neat cellulose acetate

The results of the tensile strength analysis of the CA-MCCK membrane in Fig. 6(a) demonstrated the influence of the weight percentage of MCC as a filler on the membrane's strength. The addition of MCCK at weight percentages of 0.5%, 1%, and 1.5% could enhance the tensile strength of the membrane compared to membranes without MCCK. This improvement occurred because the presence of MCCK in the polymer matrix increased compatibility by efficiently transferring stress from the cellulose acetate matrix to MCCK, thereby enhancing membrane strength [36]. Optimal tensile strength results were achieved with the addition of 1% MCCK, resulting in an increase in tensile strength from 1.13 to 1.96 $N.mm^{-2}$. However, the addition of excess MCCK, such as a weight percent of 1.5%, had a detrimental impact on reducing the tensile strength of the membrane. This was due to the diminishing quality of MCCK dispersion in the cellulose acetate polymer matrix as more MCCK was added. The decrease in dispersion quality could trigger the agglomeration of MCCK, thus affecting and reducing the tensile strength of the membrane [37].

The hydrophilicity of the CA-MCCK membrane was evaluated through the measurement of the membrane contact angle, which indicated the membrane's effectiveness in absorbing water. The results of contact angle measurements in

Fig. 6(b) illustrated the impact of incorporating MCCK into the cellulose acetate membrane matrix. Optimal outcomes were observed with the addition of 1% MCCK, leading to a decrease in the contact angle from 65 to 52°. This signified an enhancement in the hydrophilicity of the CA-MCCK membrane. This improvement was attributed to the presence of hydroxyl groups in the cellulose structure, promoting increased interaction between the membrane and water molecules [14]. The reduction in hydrophilicity observed with excess MCCK (1.5%) was attributed to an increase in solution viscosity, which tended to decrease the presence of MCCK on the membrane surface [38].

Membrane porosity is defined as the ratio between the pore volume and the total membrane volume [39]. Porosity measurements were conducted using the gravimetric method. The results of the CA-MCCK membrane porosity analysis in Fig. 6(c) illustrated the impact of adding MCCK to the cellulose acetate membrane on membrane porosity. Optimal porosity was achieved with the addition of 0.5% MCCK, leading to an increase in porosity from 82% to 85%. This rise in membrane porosity was attributed to an optimal enhancement in membrane hydrophilicity, facilitating a rapid solvent-non-solvent exchange during the phase inversion process, consequently inducing the formation of membrane pores. Barzegar et al. [40] reported that incorporating hydrophilic materials into the membrane could increase hydrophilicity, directly contributing to increased membrane porosity. However, the addition of excess MCCK resulted in a decrease in porosity due to an elevation in the viscosity of the dope solution, influencing the membrane pore formation process [41].

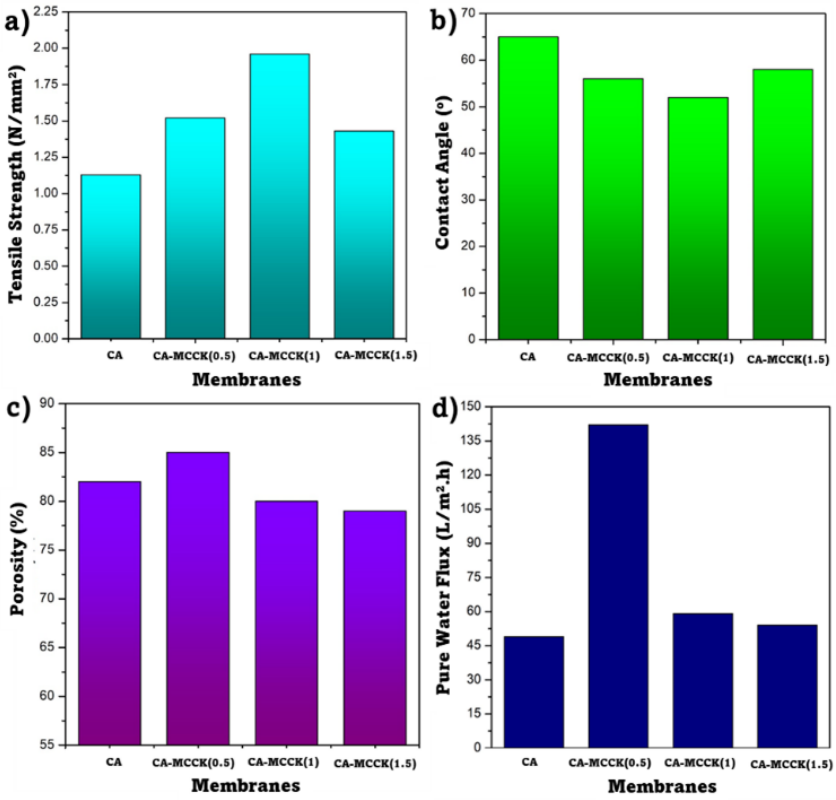

Fig. 6. (a) Tensile strength, (b) Contact angle, (c) Porosity, and (d) Pure water flux membrane CA-MCCK and neat cellulose acetate membrane

Water flux testing was conducted to assess the membrane's separation efficiency in terms of permeability, ensuring its ability to facilitate water passage during the filtration process. The addition of MCCK to the cellulose acetate membrane positively influenced the increase in water flux. Specifically, the membrane with 0.5% MCCK exhibited significantly higher water flux compared to other concentrations, surpassing even the membrane without MCCK with an increase from 49 to 142 L/m^2.h (Fig. 6(d)). This rise in water flux in the CA-MCCK membrane can be attributed to its increased hydrophilicity compared to the neat cellulose acetate membrane. The presence of hydroxyl groups in MCCK enhances membrane interactions, promoting binding with water molecules. Additionally, the increased porosity of the CA-MCCK membrane contributes to the elevated water flux, as higher membrane porosity enables the passage of more water molecules, thereby enhancing water flux.

The SEM analysis results as shown in Fig. 7 illustrated the impact of adding MCCK to the cellulose acetate matrix on changes in surface morphology structure and membrane cross-section. Fig.s 7(a)-7(f) indicate that the addition of MCC to the cellulose acetate membrane can increase the number and distribution of pores on the membrane surface. The neat cellulose acetate membrane exhibited a smoother surface with smaller and denser pore sizes, in contrast to the CA-MCCK membrane, which displayed more pore sizes and a larger diameter. This aligned with the results of membrane porosity analysis, demonstrating higher porosity in membranes with MCCK. On the other hand, the increase in water flux in the CA-MCCK membrane was also observed due to the augmentation of pores in the membrane. Fig.s 7(g)-7(l) depict a cross-section of a membrane with an asymmetrical and finger-like pore structure. The addition of MCCK to the membrane influenced the formation of larger cavities in the membrane pores. This was

attributed to MCCK agglomeration, where the size of the agglomeration formed directly correlated with the size of the cavities produced [42].

3.1. Membrane performance in dye wastewater treatment

The performance of the CA-MCCK membrane was assessed through a dye separation process using methylene blue (MB). The testing process lasted for 30 minutes with an MB concentration of 5 mg/L. The water flux test results in Fig. 8(a) demonstrated a consistent trend across the entire membrane, showing a decrease in water flux as the test time increased. This decline was attributed to fouling, which intensified with prolonged testing time. Fouling typically occurred due to the accumulation and blockage of MB molecules on the membrane surface and pores. This accumulation could lead to a reduction in membrane pore size, subsequently limiting the passage of water molecules through the membrane. Conversely, the incorporation of MCCK in cellulose acetate membranes contributed to an increase in water flux. This is a result of enhanced membrane hydrophilicity and porosity. A more hydrophilic membrane surface fostered increased interaction with water molecules through hydrogen bonds. Additionally, high membrane porosity facilitated the passage of numerous water molecules through the membrane pores [43]. The addition of 0.5% MCCK proved to be optimal in achieving enhanced water flux compared to other membrane types. This aligned with the results of porosity measurements, indicating a membrane porosity increase of up to 85%.

Fig. 8(b) presents the results of membrane performance testing against MB rejection. These findings demonstrated that the membrane with the addition of MCCK could achieve higher rejection compared to the neat cellulose acetate membrane. In pure cellulose acetate membranes, a significant decreased in MB rejection occurred as filtration time increased, with the rejection percentage dropping to 64%. Meanwhile, the membrane with MCCK filler exhibited high rejection up to 30 minutes of filtration time with a percentage reaching 99-100%.

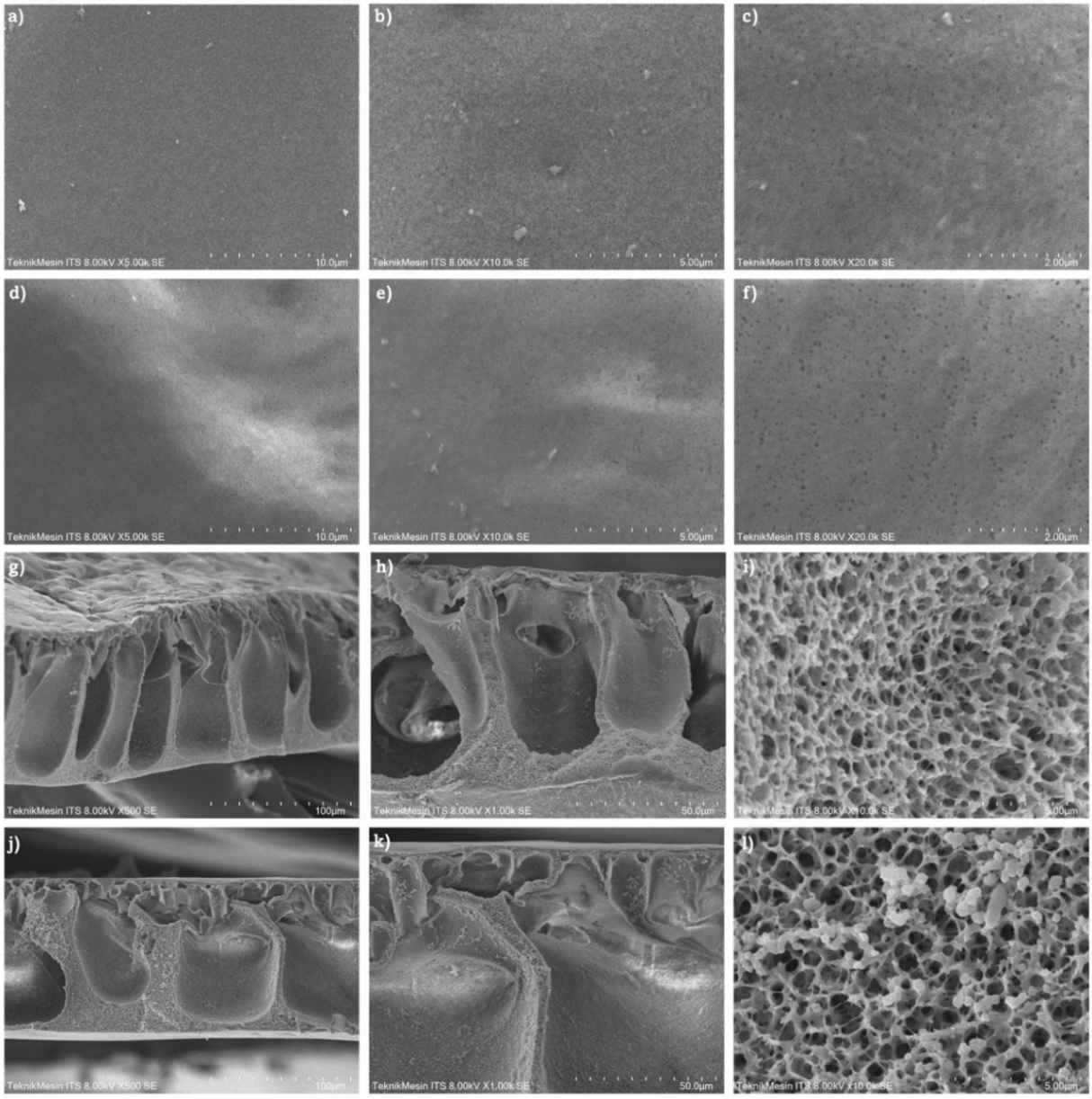

Fig. 7. The surface morphology and membrane cross sections of (a-c & g-i) CA and (d-f & j-l) CA-MCCK

This was attributed to the addition of MCCK in the cellulose acetate matrix, which increased the number of hydroxyl groups within the membrane. This, in turn, facilitated the occurrence of hydrogen bonds between the hydroxyl groups and the MB molecules. Apart from that, the possibility of agglomeration in MCCK can lead to the blockage of membrane pores, resulting in a reduction of pore size [44].

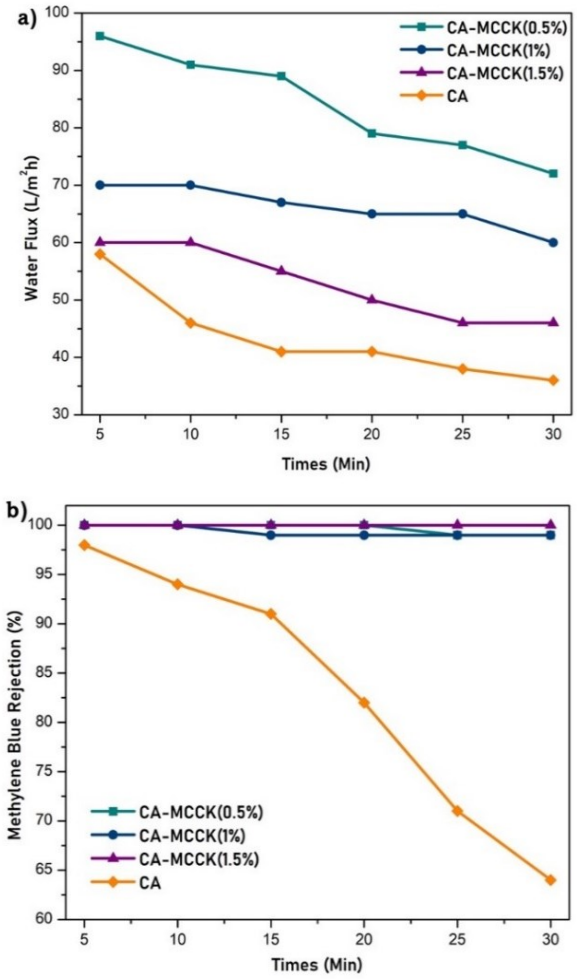

Fig. 8. (a) Water flux and (b) MB rejection of the membrane

Dye Polutants	Membrane Materials	MB Concentration (mg/L)	Membrane Performance	Reference
Methylene Blue	CA-MCCK	5	Flux = 84 L/m².h, Rejection = 99%	This Work
	CA-NAC	10	Rejection = 53%	[34]
	CA/*p*-MWCNTs	10	Rejection = 40%	[45]
	CA/MOFDPC	10	Flux = 76 L/m².h, Rejection = 94%	[46]
	CA/SnO_2	5	Rejection = 95%	[47]

4. Conclusions

An ultrafiltration membrane based on MCC filler from kapok with a cellulose acetate polymer matrix has been successfully prepared. The addition of MCCK to the membrane improved its characteristics and performance, including hydrophilicity, tensile strength, and membrane porosity. The presence of MCCK in the membrane reduced the contact angle from 65 to 52 degrees, increased membrane tensile strength from 1.13 to 1.96 N/mm², and enhanced porosity from 82 to 85%. A decrease in the contact angle indicated an increase in the hydrophilic properties of the membrane, as evidenced by an increase in pure water flux from 49 to 142 L/m².h. In MB separation, the composite membrane with MCC filler exhibited superior performance compared to the membrane without MCC with an increased water flux from 43 to 84 L/m².h and MB rejection from 64 to 99%. The use of biomass as a source of MCC is expected to increase the value of biomass utilization and produce more environmentally friendly composite membranes. Additionally, it is expected that this approach can also address wastewater issues and enhance the availability of clean water worldwide, aligning with Sustainable Development Goals (SDGs) related to clean water and sanitation (Number 6).

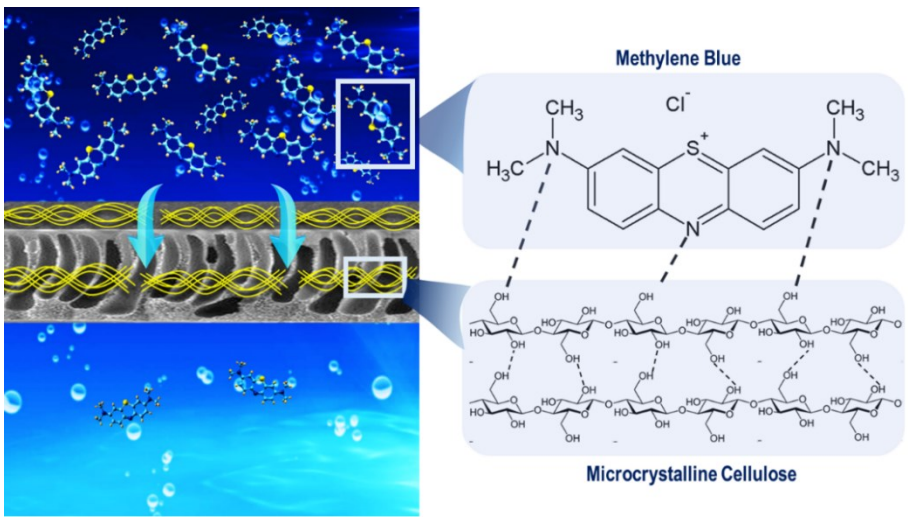

Fig. 9. Schematic of the MB separation process by the CA-MCCK membrane

Table 1. Comparison of cellulose acetate based membrane in MB separation

Acknowledgement

The authors extend their gratitude for the research funding granted by the Ministry of Education, Culture, Research, and Technology of the Republic of Indonesia under the Master's Research Towards an Excellent Undergraduate Doctorate research scheme, with contract numbers [009/E5/PG.02.00. PL/2023] and [1245/PKS/ITS/2023].

References

1. K. Harada, *Dependency of local people on the forests of Gunung Halimun National Park, West Java, Indonesia*, Tropics 13 (2003) 161–185.
2. R. Purnawati *et al.*, *Physical and chemical properties of kapok (Ceiba pentandra) and balsa (ochroma pyramidale) fibers*, J. Korean Wood Sci. Technol. 46 (2018) 393–401.
3. A. JM, *The Exploration of Alpha Cellulose in Kapok Fruit as Raw Material for Rocket Propellant Production*, Agric. Res. Technol. Open Access J. 12 (2017) 82–89.
4. D. Sartika, K. Syamsu, E. Warsiki, and F. Fahma, *Isolation of microfiber cellulose from kapok fiber (Ceiba pentandra) by using chemical-hydrothermal treatment*, Ecol. Environ. Conserv. 26 (2020) 654–662.
5. D. Sartika, K. Syamsu, E. Warsiki, F. Fahma, and I. W. Arnata, *Nanocrystalline Cellulose from Kapok Fiber (Ceiba pentandra) and its Reinforcement Effect on Alginate Hydrogel Bead*, Starch/Staerke 73 (2021) 9-10.
6. A. Sharma, M. Thakur, M. Bhattacharya, T. Mandal, and S. Goswami, *Commercial application of cellulose nano-composites–A review*, Biotechnol. Reports 21 (2019) e00316.
7. A. M. Mansora, J. S. Lima, F. N. Anib, H. Hashima, and W. S. Hoa, *Characteristics of cellulose, hemicellulose and lignin of MD_2 pineapple biomass*, Chem. Eng, 72 (2019) 79–84.
8. W. Fatriasari, N. Masruchin, and E. Hermiati, *Selulosa: Karakteristik dan Pemanfaatannya*. LIPI Press, (2019).
9. P. González-García, *Activated carbon from lignocellulosics precursors: A review of the synthesis methods, characterization techniques and applications*, Renew. Sustain. Energy Rev. 82 (2018) 1393–1414.
10. D. Klemm, B. Heublein, H. Fink, and A. Bohn, *Cellulose: fascinating biopolymer and sustainable raw material*, Angew. chemie Int. Ed. 44 (2005) 3358–3393.
11. X. Fan, Z. Liu, Z. Liu, and J. Lu, *Cellulose acetate membrane synthesis from biomass of ramie*, J. Appl. Polym. Sci. 117 (2010) 588–595.
12. Y. Jiao, C. Wan, W. Bao, H. Gao, D. Liang, and J. Li, *Facile hydrothermal synthesis of Fe_3O_4@cellulose aerogel nanocomposite and its application in Fenton-like degradation of Rhodamine B*, Carbohydr. Polym. 189 (2018) 371–378.
13. Z. Alizadeh, Z. A. Jonoush, and A. Rezaee, *Three-dimensional electro-Fenton system supplied with a nanocomposite of microbial cellulose/Fe_3O_4 for effective degradation of tetracycline*, Chemosphere 317 (2023) 137890.
14. A. I. Nazri, A. L. Ahmad, and M. H. Hussin, *Microcrystalline cellulose-blended polyethersulfone membranes for enhanced water permeability and humic acid removal*, Membranes 11 (2021) 660.
15. V. Vatanpour, M. Ağtaş, A. M. Abdelrahman, M. E. Erşahin, H. Ozgun, and I. Koyuncu, *Nanomaterials in membrane bioreactors: Recent progresses, challenges, and potentials*, Chemosphere 302 (2022) 134930.
16. M. Li, T. Wei, C. Qian, and Z. Liang, *Preparation of microcrystalline cellulose from Rabdosia rubescens residue and study on its membrane properties*, Sci. Rep. 11 (2021) 1–9.
17. I. H. Alsohaimi, A. N. Alrashidi, H. M. A. Hassan, and Q. Chen, *Highly efficient ultrafiltration membrane performance of PES@microcrystalline cellulose extracted from waste fruits for the removal of BrO_3^- from drinking water samples*, Colloids Interface Sci. Commun. 54 (2023) 100718.
18. S. Thiangtham, J. Runt, N. Saito, and H. Manuspiya, *Fabrication of biocomposite membrane with microcrystalline cellulose (MCC) extracted from sugarcane bagasse by phase inversion method*, Cellulose 27 (2020) 1367–1384.
19. E. Pramono *et al.*, *Cellulose derived from oil palm empty fruit bunches as filler on polyvinylidene fluoride based membrane for water containing humic acid treatment*, Groundw. Sustain. Dev. 17 (2022) 100744.
20. H. Holilah *et al.*, *Hydrothermal assisted isolation of microcrystalline cellulose from pepper (Piper nigrum L.) processing waste for making sustainable bio-composite*, J. Clean. Prod. 305 (2021) 127229.
21. A. M. Asiri *et al.*, *Synthesis and Characterization of Blended Cellulose Acetate Membranes*, Polymers 14 (2021) 4.
22. A. F. Owolabi, M. K. M. Haafiz, M. S. Hossain, M. H. Hussin, and M. R. N. Fazita, *Influence of alkaline hydrogen peroxide pre-hydrolysis on the isolation of microcrystalline cellulose from oil palm fronds*, Int. J. Biol. Macromol. 95 (2017) 1228–1234.
23. P. N. Trisant, I. Gunardi, and Sumarno, *The Influence of Hydrolysis Time in Hydrothermal Process of Cellulose from Sengon Wood Sawdust*, Macromol. Symp. 391 (2020) 1–5.
24. D. Sartika, K. Syamsu, E. Warsiki, and F. Fahma, *Optimization of Sulfuric Acid Concentration and Hydrolysis Time on Crystallinity of Nanocrystalline Cellulose : A Response Surface Methodology Study*, IOP Conf. Ser. Earth Environ. Sci. 355 (2019) 012109.
25. P. Chaudhary, K. M. Rao, S. M. Choi, S. Zo, M. Suneetha, and S. S. Han, *Tannic Acid-chitosan Strengthened Cellulose Filter Paper for Water Disinfection via Formation of Silver Nanoparticles*, Fibers Polym. 22 (2021) 2979–2985.
26. W. R. Kunusa, R. Abdullah, K. Bilondatu, and W. Z. Tulie, *Analysis of Cellulose Isolated from Sugar Bagasse: Optimization and Treatment Process Scheme*, Journal of Physics: Conference Series (2020) 012040.
27. D. K. Jindal and S. K. Singh, *Synthesis, ftir and 1 h-nmr characterization of chitin acetate/succinate mixed esters*, Pharmanest 7 (2016) 3134–3139.
28. E. Mayasari, S. Fukugaichi, E. Johan, and N. Matsue, *Low-energy extraction of lignocellulose nanofibers from fresh Musa basjoo pseudo-stem*, Commun. Sci. Technol. 8 (2023) 108–112.
29. M. Carrier *et al.*, *Thermogravimetric analysis as a new method to determine the lignocellulosic composition of biomass*, Biomass and Bioenergy 35 (2011) 298–307.
30. T. Zhao, Z. Chen, X. Lin, Z. Ren, B. Li, and Y. Zhang, *Preparation and characterization of microcrystalline cellulose (MCC) from tea waste*, Carbohydr. Polym. 184 (2018) 164–170.
31. Yusnimar, Evelyn, A. Aman, Chairul, S. Rahmadahana, and A. Amri, *Manufacturing of high brightness dissolving pulp from sansevieria-trifasciata fiber by effective sequences processes*, Commun. Sci. Technol. 7 (2022) 45–49.
32. A. Jamil *et al.*, *Development and Performance Evaluation of Cellulose Acetate-Bentonite Mixed Matrix Membranes for CO_2 Separation*, Adv. Polym. Technol. 2020 (2020) 8855577.
33. K. Xu *et al.*, *Green sustainable, facile nitrogen self-doped porous carbon derived from chitosan/cellulose nanocrystal biocomposites as a potential anode material for lithium-ion batteries*, J. Taiwan Inst. Chem. Eng. 109 (2020) 79–89.
34. O. A. Koriem, A. M. Kamel, W. Shaaban, and M. F. Elkady, *Enhancement of Dye Separation Performance of Eco-Friendly Cellulose Acetate-Based Membranes*, Sustain. 14 (2022) 14665.
35. D. Marlina, M. Novita, M. T. Anwar, H. Kusumo, and H. Sato, *Raman spectra of polyethylene glycol/cellulose acetate butyrate biopolymer blend*, J. Phys. Conf. Ser. 1869 (2021) 012006.
36. H. Yousefian and D. Rodrigue, *Hybrid Composite Foams Based on Nanoclays and Natural Fibres*, in *Nanoclay Reinforced Polymer Composites*, Springer 2016 (2016) 51–79.
37. H. Bai, X. Wang, Y. Zhou, and L. Zhang, *Preparation and*

characterization of poly(vinylidene fluoride) composite membranes blended with nano-crystalline cellulose, Prog. Nat. Sci. Mater. Int. 22 (2012) 250–257.

38. H. Bai, Y. Zhou, and L. Zhang, *Morphology and Mechanical Properties of a New Nanocrystalline Cellulose/Polysulfone Composite Membrane*, Adv. Polym. Technol. 34 (2015).
39. D. R. Amiyati, D. Indarti, and Y. M. Muflihah, *Pengaruh Variasi Waktu Penguapan Terhadap Kinerja Membran Selulosa Asetat pada Proses Ultrafiltrasi*, Berk. Sainstek 5 (2017) 7.
40. H. Barzegar, M. A. Zahed, and V. Vatanpour, *Antibacterial and antifouling properties of Ag3PO4/GO nanocomposite blended polyethersulfone membrane applied in dye separation*, J. Water Process Eng. 38 (2020) 101638.
41. H. Tu, X. Li, Y. Liu, L. Luo, B. Duan, and R. Zhang, *Recent progress in regenerated cellulose-based fibers from alkali/urea system via spinning process*, Carbohydr. Polym. 296 (2022) 119942.
42. S. Wang, A. Lu, and L. Zhang, *Recent advances in regenerated cellulose materials*, Prog. Polym. Sci. 53 (2016) 169–206.
43. R. Abdullah *et al.*, *Fabrication of composite membrane with microcrystalline cellulose from lignocellulosic biomass as filler on cellulose acetate based membrane for water containing methylene blue treatment*, Bioresour. Technol. Reports 25 (2024) 101728.
44. T. van den Berg and M. Ulbricht, *Polymer Nanocomposite Ultrafiltration Membranes: The Influence of Polymeric Additive, Dispersion Quality and Particle Modification on the Integration of Zinc Oxide Nanoparticles into Polyvinylidene Difluoride Membranes*, Membranes 10 (2020) 197.
45. M. A. Silva, L. Hilliou, and M. T. P. de Amorim, *Fabrication of pristine-multiwalled carbon nanotubes/cellulose acetate composites for removal of methylene blue*. Springer Berlin Heidelberg 77 (2020) 623-653.
46. S. Tahazadeh, T. Mohammadi, M. A. Tofighy, S. Khanlari, H. Karimi, and H. B. Motejadded Emrooz, *Development of cellulose acetate/metal-organic framework derived porous carbon adsorptive membrane for dye removal applications*, J. Memb. Sci. 638 (2021) 119692.
47. F. Costantino, A. Armirotti, R. Carzino, L. Gavioli, A. Athanassiou, and D. Fragouli, *In situ formation of SnO_2 nanoparticles on cellulose acetate fibrous membranes for the photocatalytic degradation of organic dyes*, J. Photochem. Photobiol. A Chem. 398 (2020) 112599.